

Evolution of Coherence and Superconductivity in Electron-Doped Cuprates

G. Blumberg*, M.M. Qazilbash†, B.S. Dennis* and R.L. Greene†

*Bell Laboratories, Lucent Technologies, Murray Hill, NJ 07974, USA

†Department of Physics, University of Maryland, College Park, MD 20742, USA

Abstract. The superconducting (SC) phase diagram of the electron-doped cuprates has been explored by Raman spectroscopy as a function of doping x , temperature T , and magnetic field H . The data is consistent with *nonmonotonic* SC order parameter (OP) of the d -wave form. The persistence of SC coherence peaks in the B_{2g} channel for all dopings implies that superconductivity is mainly governed by interactions in the vicinity of $(\pm\pi/2a, \pm\pi/2a)$ regions of the Brillouin zone. Effective upper critical field lines $H_{c2}^*(T, x)$ at which the superfluid stiffness vanishes and $H_{c2}^{\Delta}(T, x)$ at which the SC amplitude is suppressed by field have been determined. The difference between the two quantities suggests the presence of phase fluctuations that increase for $x < 0.15$. It is found that the field suppresses the magnitude of the SC gap linearly at an anomalously large rate. H_{c2}^{Δ} value that is about 10 T for optimally doped samples decreases below a Tesla for overdoped cuprates.

Keywords: Superconductivity, Raman Scattering, Magnetic Field

PACS: 74.25.Ha, 74.25.Gz, 74.72.-h, 78.30.Er

We use electronic Raman spectroscopy to study quasiparticle (QP) spectra renormalization in magnetic fields on single crystals and films of $\text{Pr}_{2-x}\text{Ce}_x\text{CuO}_{4-\delta}$ (PCCO) and $\text{Nd}_{2-x}\text{Ce}_x\text{CuO}_{4-\delta}$ (NCCO) with different Ce doping covering most of the SC phase diagram. We find that the SC gap magnitude is strongly suppressed in magnetic fields. From the temperature and doping dependence of the SC coherence peak, we extract an effective upper critical field line $H_{c2}^*(T, x)$ at which the superfluid stiffness vanishes. Field dependence of the measured SC gap value reveals an estimate of $H_{c2}^{\Delta}(T, x)$, an upper critical field at which the SC amplitude is completely suppressed by field. We find that ξ_{GL} increases from 60 Å for optimal doping (OPT) to 220 Å for the most overdoped (OVD) sample with $T_c = 13$ K. For the latter case $k_F \xi_{GL} \approx 150$ is much larger than for p -doped cuprates but is still not reaching the regime of conventional BCS-like tightly overlapping Cooper pairs.

In the SC state, the strength of the low-frequency Raman scattering intensity in the normal state is reduced and the spectral weight moves to the 2Δ coherence peak resulting from excitations out of the SC condensate (Fig. 1). In the B_{2g} and A_{1g} channels, the “pair-breaking” SC coherence peaks appear for all dopings while in the B_{1g} channel these SC coherence peaks are negligibly weak in the underdoped (UND) and the most OVD films. For the OPT crystal, the SC coherence peak energy is larger in the B_{2g} channel compared with that in B_{1g} . The intensity below the SC coherence peaks vanishes smoothly without a threshold to the lowest frequency measured. The smooth decrease in the Raman response

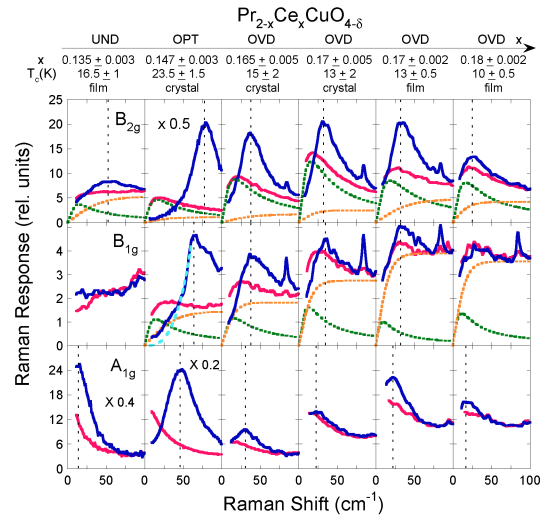


FIGURE 1. Doping dependence of the low energy electronic Raman response of PCCO single crystals and films for B_{2g} , B_{1g} and A_{1g} channels obtained with 647 nm excitation. The columns are arranged from left to right in order of increasing cerium doping. The light curves are the data taken just above the respective T_c of the samples. The normal state response in the B_{2g} and B_{1g} channels is decomposed into a coherent Drude-like contribution and an incoherent continuum (dotted lines). The dark curves show the data taken in the superconducting state at $T \approx 4$ K. The dashed vertical lines indicate positions of the SC coherence peaks.

below the SC coherence peak was interpreted in terms of a *nonmonotonic* d -wave OP with nodes along the $(0,$

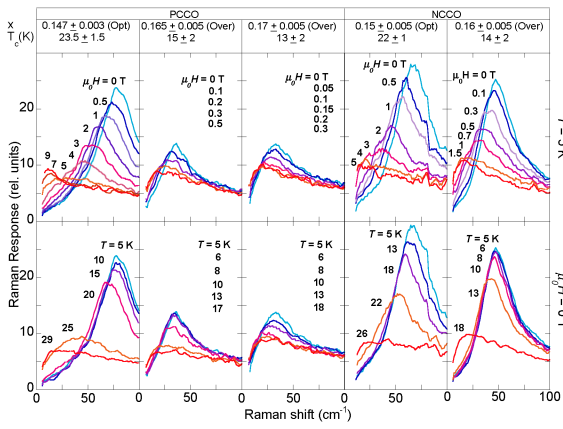


FIGURE 2. Raman response function for 647 nm excitation and right-left (RL) polarization for five single crystals of PCCO and NCCO with different Ce dopings x . The first row shows the disappearance of the 2Δ coherence peak in increasing magnetic field applied normal to the ab -plane of the crystals at 5 K. The second row shows the temperature dependence of the 2Δ peak in zero magnetic field.

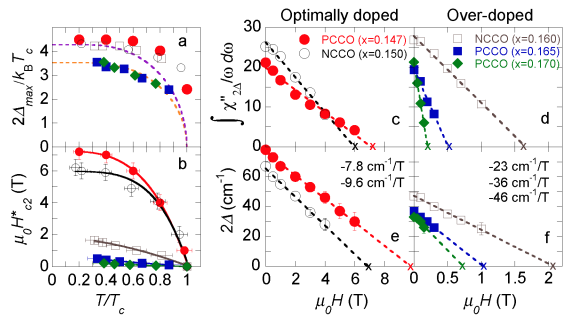


FIGURE 3. Temperature and field dependence of the SC OP amplitude and stiffness for two NCCO (open symbols) and three PCCO (filled symbols) single crystals. The temperature dependence (a) of the reduced SC gap magnitude at zero field, and (b) of the effective upper critical field H_{c2}^* that completely suppresses the SC coherence peak intensity at the given temperature. The field dependence at 5 K of the integrated coherence intensity $\int \chi''_{2\Delta}(\omega)/\omega d\omega$ is shown in panels (c) and (d) and the SC coherence peak energy (2Δ) in panels (e) and (f) for OPT and OVD crystals correspondingly. Approximated from the data effective upper critical fields H_{c2}^* and the values of the SC gap collapse $H_{c2}^{2\Delta}$ are indicated with "x". Panels (e) and (f) include also the rate of the gap suppression $\frac{d2\Delta(H)}{dH}$.

$0) \rightarrow (\pi/a, \pi/a)$ diagonal and the maximum gap being closer to this diagonal than to the BZ boundaries.

Fig. 2 exhibits the field and temperature dependence of the SC coherence peak at the maximum gap value ($2\Delta_{max}$) for the OPT ($x \approx 0.15$) and OVD ($x > 0.15$) PCCO and NCCO crystals. The coherence peak loses intensity and moves to lower energies by either increasing the temperature or magnetic field. We define an effective

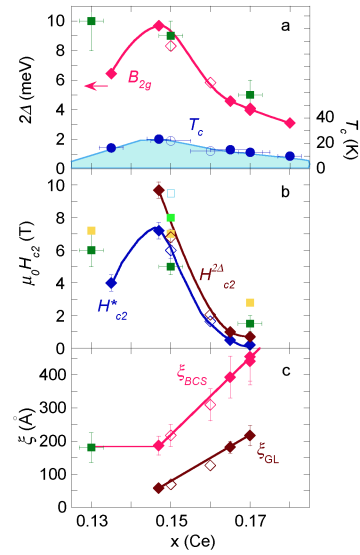


FIGURE 4. Phase diagram of PCCO (filled diamonds) and NCCO (open diamonds) superconductors explored by electronic Raman scattering in magnetic field. Panels show: (a) T_c (circles), the maximum energy of the SC 2Δ coherence peak and the distance between coherence peaks from point contact tunneling spectroscopy (squares); (b) The doping dependence at 5 K of the effective upper critical fields $H_{c2}^*(x)$ and the fields suppressing the gap amplitude $H_{c2}^{2\Delta}(x)$ is compared to upper critical fields obtained from other measurements (squares) including point contact tunneling, Nernst effect, and thermal conductivity; (c) the Ginzburg-Landau SC coherence length $\xi_{GL}(x) = \sqrt{\Phi_0/2\pi H_{c2}^{2\Delta}(x)}$ is compared to the BCS coherence length $\xi_{BCS}(x) = \hbar v_F / \pi \Delta_{max}(x)$ obtained from the Raman gap data. All solid lines are guides to the eye.

upper critical field, $H_{c2}^*(T, x)$, as the field that completely suppresses the coherence peak intensity (See Fig. 3). Reduced gap values and effective upper critical fields as a function of the reduced temperature for five single crystals of various doping levels are plotted in Figs. 3a-3b. For the lowest measured temperature, $2\Delta_{max}/k_B T_c$ values fall between 4.5 for the OPT crystals and 3.5 for the most OVD crystals. In Fig. 4 we show that the fields suppressing the gap amplitude, $H_{c2}^{2\Delta}(x)$, are related to the SC gap magnitude.

ξ_{GL} for the n -doped cuprates is significantly larger than for their p -doped counterparts and that leads to important differences. First, the size of the Cooper pair is much larger than the average inter-particle spacing: $k_F \xi_{GL}$ ranges between 40 and 150. Second, a larger Cooper pair size requires further pair interactions to be taken into account and leads to a more complicated non-monotonic momentum dependence of the SC gap than the simplest d -wave form $\Delta(\mathbf{k}) \propto \cos(k_F x a) - \cos(k_F y a)$ that well describes the gap function for p -doped cuprates with tight Cooper pairs.